Reactive and Functional Polymers 160 (2021) 104831

Contents lists available at ScienceDirect

Reactive and Functional Polymers

journal homepage: www.elsevier.com/locate/react

Perspective Article

Immobilization of copper(II) into polyacrylonitrile fiber toward efficient and recyclable catalyst in Chan-Lam coupling reactions

Chenlu Zhang [a,1], Hai Zhu [a,1], Kaiyue Gang [b], Minli Tao [a], Ning Ma [a,*], Wenqin Zhang [a,c]

[a] *Department of Chemistry, School of Science, Tianjin University, Tianjin 300072, PR China*
[b] *School of Chemical Engineering, Tianjin University, Tianjin 300072, PR China*
[c] *Key Laboratory of Inorganic-Organic Hybrid Functional Materials Chemistry, Ministry of Education, Tianjin Key Laboratory of Structure and Performance for Functional Molecules, Tianjin Normal University, Tianjin 300387, PR China*

ARTICLE INFO

Keywords:
Polyacrylonitrile fiber
Heterogeneous copper catalysis
Chan-Lam coupling
N-Arylimidazole
N-Arylsulfonamide

ABSTRACT

A series of polyacrylonitrile fiber (PANF)-supported copper(II) catalysts were prepared through the immobilization of Cu(II) into prolinamide-modified PANF ($PAN_{PA\text{-}2}F$) and subsequently used for the synthesis of diverse *N*-arylimidazoles from arylboronic acids and imidazole. The prepared Cu(II)@$PAN_{PA\text{-}2}$Fs were well characterized by mechanical strength, FT-IR, XRD, XPS and SEM. Among them, $CuCl_2$@$PAN_{PA\text{-}2}F$ exhibited excellent catalytic performance, and its activity was significantly affected by the Cu loading. This catalytic system also displayed good activity in the synthesis of *N*-arylsulfonamides from arylboronic acids and tosyl azide. It was highly efficient in gram-scale reactions and could be reused five times. The advantages of low cost, easy preparation, good durability and facile recovery make the fiber catalyst attractive.

1. Introduction

Transition metal-catalyzed carbon-nitrogen couplings have been powerful for the production of amine, amide and *N*-heterocycle in a wide range of pharmaceuticals, natural products, dyes and functional materials [1–3]. Of these nitrogen-containing compounds, *N*-arylimidazoles have attracted significant interest because of their bioactivities such as anti-inflammatory [4], antifungal [5], and analgesic [6]. Moreover, the alkylation of imidazole moiety provides diverse ionic liquids which were involved in organic transformations as environmental friendly solvents and catalysts [7,8]. The tautomeric structure of imidazole unit also expands its synthetic utilities as precursor to *N*-heterocyclic carbenes [9,10], which acted as organocatalysts and excellent ligands in metal catalysis [11]. More recently, the imidazole unit was found in organic conjugated polymers for the application as electroluminescent devices, sensors, and other semiconductor devices [12,13].

Numerous protocols for C—N coupling to prepare *N*-arylimidazole have been proposed over past decades, including nucleophilic aromatic substitution of imidazole [14] and Ullmann cross-couplings of aryl halide with imidazole [15–19]. These methods usually show acceptable efficiency, yet, some apparent drawbacks such as high reaction temperature, long reaction time and poor substrate generality reduce their attractiveness in organic synthetic chemistry. Since the pioneering works reported by Chan and Lam, Cu-catalyzed coupling of arylboronic acids with imidazole (Chan-Lam coupling) has gained a lot of interest owing to its mild reaction conditions (room temperature and weak base) [20,21]. A large number of reports have been proposed about the modification and extension of this reaction, but the development of simpler and more versatile catalytic system is still highly desired [22–27].

Despite tremendous progress in homogeneous copper-catalyzed Chan-Lam coupling, the intrinsic disadvantages of homogeneous catalysis such as the complicated separation of metal catalyst and non-reusability remain unsolved, which inevitably cause the environmental pollution and hamper its utility from laboratory scale to chemical production. In this context, heterogenization of homogeneous catalyst onto stable solid support simplifies the reclaiming of catalyst, and ultimately leads to simple, economical, environmentally benign and sustainable process. Recently, many solid materials such as silica [28], graphene [29], organic polymers [30,31], metal-organic frameworks [32,33], covalent-organic frameworks [34], and magnetic nanoparticles [35] have been used as supports for copper catalysts in Chan-Lam coupling. These heterogeneous catalysts were typically present as

---

* Corresponding author.
E-mail address: mntju@tju.edu.cn (N. Ma).

[1] Both authors contributed equally to this work.

https://doi.org/10.1016/j.reactfunctpolym.2021.104831
Received 9 October 2020; Received in revised form 20 January 2021; Accepted 22 January 2021

small particles or powders, which could enhance their contact area between reactants and catalytic sites during heterogeneous catalysis. However, the recovery of such heterogeneous catalysts might be tedious and time-consuming because of the formed pressure drop in filtration.

Polyacrylonitrile fiber (PANF), an artificial synthetic polymer material, has recently attracted much attention due to its low density, excellent flexibility, high thermal stability and good solvent resistance. These properties facilitate the modification of fiber through covalent bonding into desirable polymer support. Especially, the cyano and ester groups in PANF could be partially converted to other functional groups via aminolysis and hydrolysis, which provide a variety of opportunities toward the design of novel absorbents and heterogeneous catalysts. Fiber-immobilized absorbents have been widely applied to the removal of heavy metal ions [36] or organic pollutants [37,38], and the separation and recovery of noble metal [39] from waste water directly and effectively. Several groups including us have reported that fiber materials, especially PANF, could be modified into not only supported acid [40] and base [41,42], but also immobilized metal catalysts for organic reactions [43,44], with excellent catalytic performance and prominent applicability. It is worth to note that, compared with other solid materials with rigid matrix, flexible structure of fiber ensures its stretching and rotation, thus improving the mass diffusion and making the catalytic sites accessible to the reactants adequately. In addition, the regular and flexible structure of fiber material also facilitated its quick and convenient separation by filtration from reaction system.

As a non-toxic natural amino acid, proline has been extensively employed as organocatalyst in various organic reactions because of its low price, stability under air and moisture, and highly catalytic activity [45–47]. The presence of adjacent amino and carboxy groups make proline and its derivatives good ligands in transition metal catalysis [48,49]. For example, Alper et al. prepared MNPs-supported proline as reusable ligand for Cu-catalyzed arylation of nitro nucleophiles [50]. You et al. reported proline ionic liquid anchored on polystyrene showed good reactivity and recyclability for Cu-catalyzed *N*-arylation [51]. Recently, Iglesias et al. presented that copper and rhodium complexes immobilized on porous aromatic frameworks with prolinamide ligand exhibited high activity in cyclopropanation, A3 coupling and hydrogenation reactions [52]. In our earlier report, we described that prolinamide-functionalized PANF was prepared from the easily available L-proline methyl ester hydrochloride and used as efficient catalyst for Knoevenagel and the related multicomponent reactions in water [53]. Encouraged by all the above-mentioned investigations, herein we propose that compared with PANF, the prolinamide-modified PANF has enhanced affinity to Cu(II) ion due to the chelation function of prolinamide moiety, which will make Cu ions more easily accumulate and reside in its surface microenvironment so that Cu(II) ions could be immobilized efficiently. Thus, the novel microenvironment with active Cu sites and the appropriate adjacent hydrophobic moieties can be constructed as active and recyclable catalytic system for base-free Chan-Lam coupling.

2. Results and discussion

2.1. Preparation of fiber immobilized copper catalysts

The preparation of fiber-immobilized copper catalyst ($\mathrm{CuCl_2}$@PAN$_{\mathrm{PA\text{-}2}}$F) was shown in Scheme 1. Prolinamide-modified fiber PAN$_{\mathrm{PA\text{-}2}}$F was prepared from PANF and prolinamide derivative ((*S*)-*N*-(2-aminoethyl)pyrrolidine-2-carboxamide) according to our reported procedure [53] with slight modification (for detailed preparation of prolinamide derivative, see Supporting Information). The functional degree of PAN$_{\mathrm{PA\text{-}2}}$F was calculated by the equation as follows: functional degree $= ((w_2\text{-}w_1)/(w_2 \times \Delta \mathrm{M})) \times 1000$, where w_1 and w_2 are the weights of fiber before and after modification, respectively, and ΔM is the changed molecular weight of fiber. Then PAN$_{\mathrm{PA\text{-}2}}$F was used to immobilize copper salts in water at room temperature to afford the corresponding fiber-immobilized copper material (Cu(II)@PAN$_{\mathrm{PA\text{-}2}}$F), in which the Cu content (Cu loading) was determined by atomic absorption spectrometry (AAS) (Table 1). By balancing the functional degree and mechanical strength, the PAN$_{\mathrm{PA\text{-}2}}$F with functional degree of 1.15 mmol g^{-1} was generally used unless otherwise specified, which gave the Cu loading of 0.90 mmol g^{-1}. Mechanical strength test, FT-IR, XRD, TGA, XPS, SEM and AAS were further employed for the characterization of Cu(II)@PAN$_{\mathrm{PA\text{-}2}}$Fs.

2.2. Characterization of fiber-immobilized copper catalyst

The mechanical properties of different Cu(II)@PAN$_{\mathrm{PA\text{-}2}}$Fs were measured by mechanical strength test and the results are summarized in Table S1. The breaking strength $\mathrm{CuCl_2}$@PAN$_{\mathrm{PA\text{-}2}}$F, $\mathrm{Cu(OAc)_2}$@PAN$_{\mathrm{PA\text{-}2}}$F and $\mathrm{CuSO_4}$@PAN$_{\mathrm{PA\text{-}2}}$F had only 0.08, 0.1 and 0.07 cN loss compared with the parent PAN$_{\mathrm{PA\text{-}2}}$F (8.52 cN), respectively, which showed their good mechanical stability.

The FT-IR spectra of different fibers are shown in Fig. 1. For original PANF, the strong absorption peak at 2245 cm^{-1} is caused from stretching vibration of C≡N group, and the sharp peak at 1733 cm^{-1}

Table 1
The copper contents of the functionalized fibers.

Entry	Fiber	Cu content (mmol g^{-1})[a]
1	PANF	–
2	PAN$_{\mathrm{PA\text{-}2}}$F	–
3	$\mathrm{CuCl_2}$@PAN$_{\mathrm{PA\text{-}2}}$F	0.90
4	$\mathrm{Cu(OAc)_2}$@PAN$_{\mathrm{PA\text{-}2}}$F	0.84
5	$\mathrm{CuSO_4}$@PAN$_{\mathrm{PA\text{-}2}}$F	0.83
6[b]	$\mathrm{CuCl_2}$@PAN$_{\mathrm{PA\text{-}2}}$F	0.54
7[c]	$\mathrm{CuCl_2}$@PAN$_{\mathrm{PA\text{-}2}}$F	0.68
8[d]	$\mathrm{CuCl_2}$@PAN$_{\mathrm{PA\text{-}2}}$F	1.07

[a] Determined by atomic absorption spectrometry; [b,c,d] The functional degree of PAN$_{\mathrm{PA\text{-}2}}$F is 0.74, 0.93 and 1.39 mmol g^{-1}, respectively.

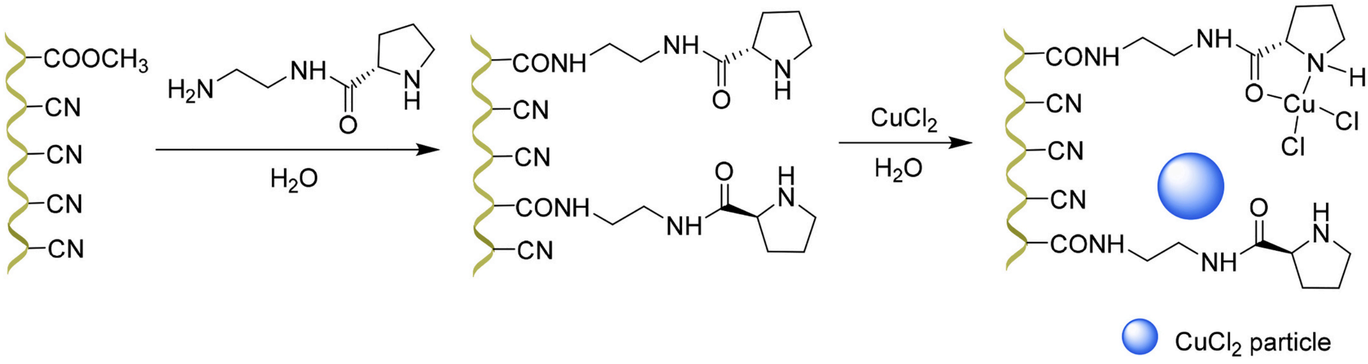

Scheme 1. The preparation of $\mathrm{CuCl_2}$@PAN$_{\mathrm{PA\text{-}2}}$F.

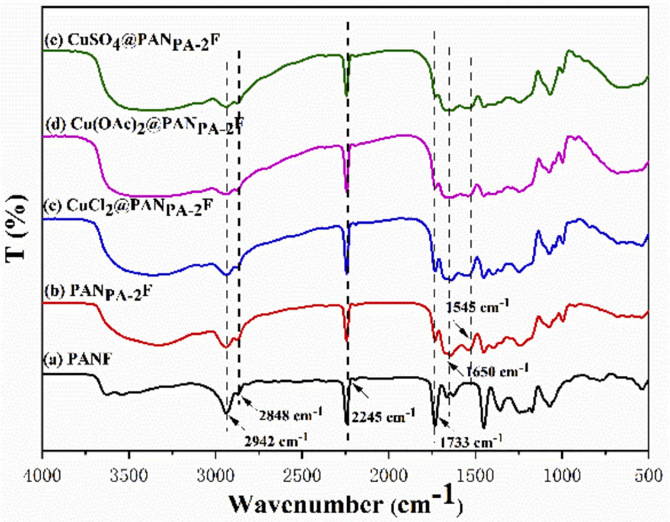

Fig. 1. The FT-IR spectra of (a) PANF, (b) PAN$_{PA-2}$F, (c) CuCl$_2$@PAN$_{PA-2}$F, (d) Cu(OAc)$_2$@PAN$_{PA-2}$F and (e) CuSO$_4$@PAN$_{PA-2}$F.

belongs to C=O stretching vibration of the methoxycarbonyl. The absorption peaks at 2942 cm^{-1} and 2848 cm^{-1} are ascribed to the stretching vibrations of -CH$_2$ group of fiber backbone. After the grafting of prolinamide moiety, the relative intensity of peak related to C=O group decreased considerably, which indicated the ester moiety was consumed during the aminolysis process. And two new peaks at 1660 and 1545 cm^{-1} corresponding to amide I (C=O stretching vibration in CONHs) and amide II (N—H bending vibration in CONHs) were observed, respectively. After the immobilization of Cu(II) salts into PAN$_{PA-2}$F, the characterization peaks of CuCl$_2$@PAN$_{PA-2}$F, Cu(OAc)$_2$@PAN$_{PA-2}$F and CuSO$_4$@PAN$_{PA-2}$F showed no distinct change from the parent PAN$_{PA-2}$F. This may be because the Cu salts were mainly adsorbed physically in fiber and the chelation of prolinamide moiety was weak; also, the contents of adsorbed Cu salts were not high enough to make the IR spectra changed obviously. This observation is consistent with the previously reported result of amine functionalized fiber-supported CuI [54].

The stability of fiber catalyst is an important factor for their practical application. Therefore, the thermal behavior of different fiber was investigated by TGA in nitrogen atmosphere from room temperature to 800 °C. The TGA curve of original PANF shows the fiber material can be stable up to 315 °C (Fig. 2a). After modification, the TGA curves of PAN$_{PA-2}$F, CuCl$_2$@PAN$_{PA-2}$F, Cu(OAc)$_2$@PAN$_{PA-2}$F and CuSO$_4$@PAN$_{PA-2}$F display the similar two-step thermal decomposition. For CuCl$_2$@PAN$_{PA-2}$F, slight weight loss before 125 °C is likely due to the removal of physically absorbed water, whereas a main weight loss in the range of 150 to 500 °C is related to the decomposition of organic moiety grafted on the surface of fiber. Additionally, the DTG curves of fiber show that CuCl$_2$@PAN$_{PA-2}$F is more stable than the other two fiber-supported copper catalysts because of its slower rate of decomposition (Fig. 2b). Although a slight decrease of initial decomposition temperature of all functionalized fibers was observed in comparison with original PANF, it is sufficient for their employment in organic transformation performed in this study.

The solvent resistance of PAN$_{PA-2}$F and CuCl$_2$@PAN$_{PA-2}$F was investigated by immersing the fiber in different solvents such as H$_2$O, MeOH, EtOH, CH$_3$CN, EtOAc and CH$_2$Cl$_2$ for 24 h at room temperature. After that, the fibers were filtered, washed completely with EtOH, and dried overnight at 60 °C under vacuum. No mass change was observed between the treated and fresh fibers, and the unchanged FT-IR spectra of the treated fibers also confirmed their structural stability, which indicates that fiber catalysts have desired solvent resistance.

The XRD patterns of PANF, PAN$_{PA-2}$F, CuCl$_2$@PAN$_{PA-2}$F, Cu(OAc)$_2$@PAN$_{PA-2}$F and CuSO$_4$@PAN$_{PA-2}$F are shown in Fig. 3a. For original PANF, the strong reflection peaks at 17.0° is related to (100) diffraction of the hexagonal lattice planes formed by the parallelly and closely packed molecule rods. Due to the intramolecular dipole-dipole interactions between nitrile groups, the molecular chain of PANF is of the irregular helical conformation. This diffraction peak was well maintained in the XRD pattern of PAN$_{PA-2}$F, indicating such modification did not significant affect the basic crystal lattice. A new peak was clearly observed in the XRD pattern of CuCl$_2$@PAN$_{PA-2}$F at 15.8°, which corresponds to (1 1 0) lattice plane of CuCl$_2$ [55]. This result demonstrates the successful immobilization of Cu(II) into the fiber (Fig. 3a–b). Moreover, the XPS spectra of different fibers are displayed in Fig. 3c–d. The main signals of O1s, N1s, C1s, Cl 2p and Cu 2p can be clearly observed in CuCl$_2$@PAN$_{PA-2}$F at 532.6, 400.4v, 285.4, 199.0 and 953–934 ev, respectively (Fig. 3c). As shown in Fig. 3d, two signals related to Cu 2p 1/2 and 2p 3/2 are centered at 953.7 and 934.8 ev, respectively, along with the corresponding peaks at 938.9–945.5 ev. These peaks are the features of divalent Cu cation [56], indicating the oxidation state of metal does not change after immobilization. In the spectra of Cu(OAc)$_2$@PAN$_{PA-2}$F and CuSO$_4$@PAN$_{PA-2}$F, these characterization signals were also clearly visible (Fig. S1a-b).

The surface morphology of fiber was observed by SEM and their images are show in Fig. 4. For original PANF, the surface of fiber was flat, smooth and uniform with an average diameter of about 23 μm. After the modification by prolinamide, the shape of fiber kept well and its morphology was nearly unchanged. Additionally, the fiber-supported copper catalysts maintained good integrity of the fiber material and no obvious crack or degradation was observed. EDX spectrum was also conducted to determine the presence of Cu in the CuCl$_2$@PANPA-2F

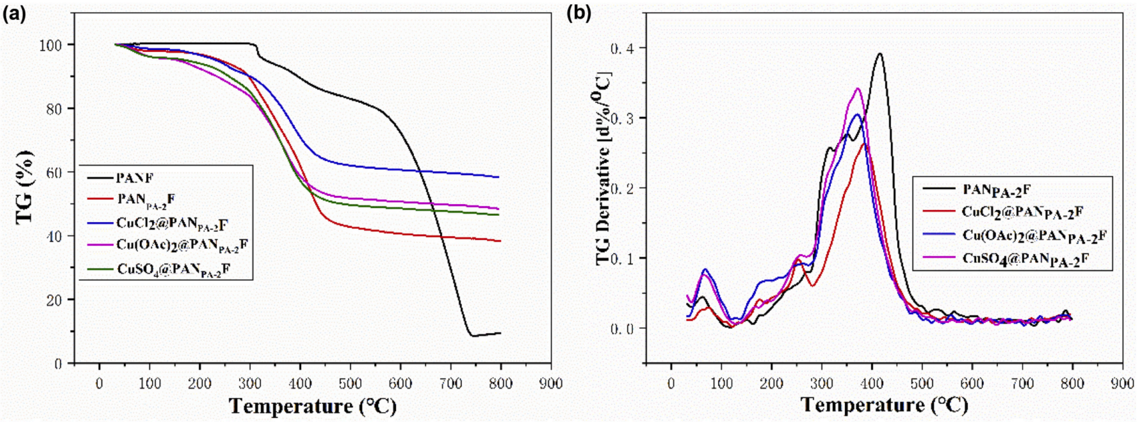

Fig. 2. The (a) TG and (b) DTG curves of PANF, PAN$_{PA-2}$F, CuCl$_2$@PAN$_{PA-2}$F, Cu(OAc)$_2$@PAN$_{PA-2}$F and CuSO$_4$@PAN$_{PA-2}$F.

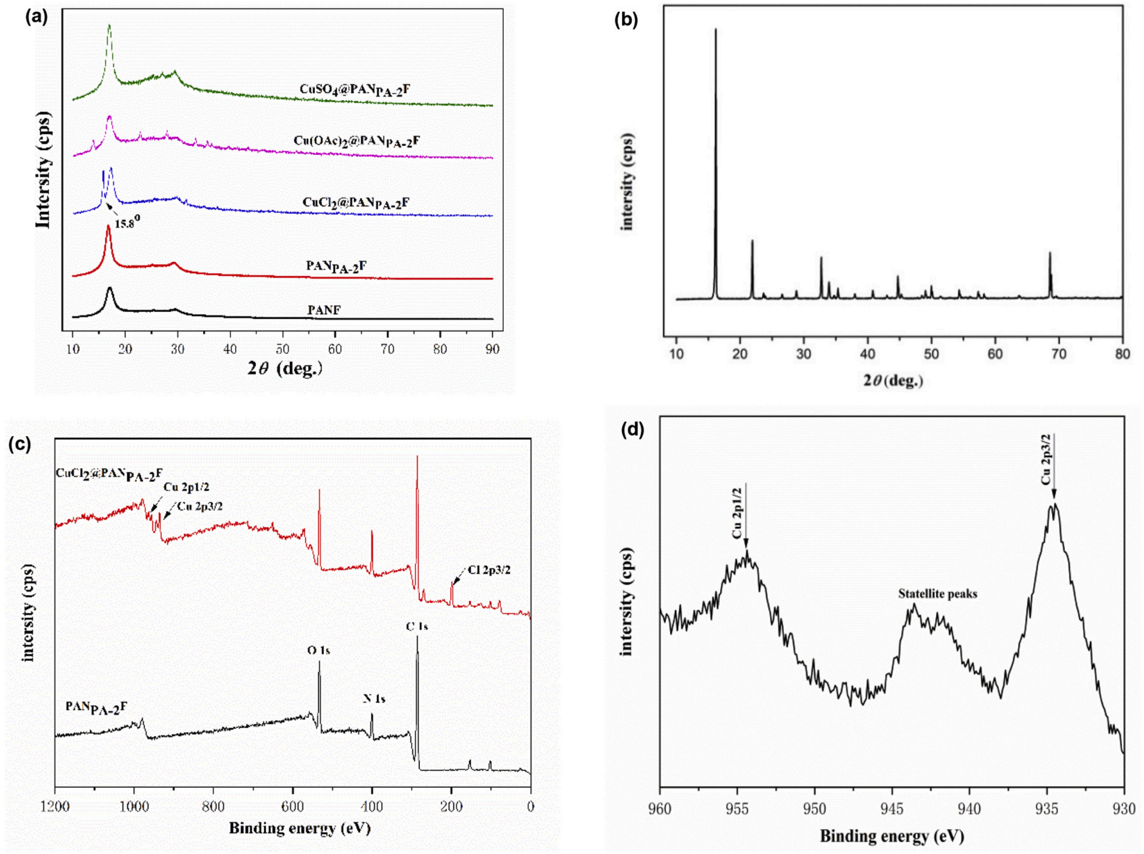

Fig. 3. The XRD curves of (a) PANF, PAN$_{PA-2}$F, CuCl$_2$@PAN$_{PA-2}$F, Cu(OAc)$_2$@PAN$_{PA-2}$F, CuSO$_4$@PAN$_{PA-2}$F and (b) $CuCl_2 \cdot 2H_2O$; The XPS spectra of (c) CuCl$_2$@PAN$_{PA-2}$F, (d) CuCl$_2$@PAN$_{PA-2}$F in the region of Cu 2p.

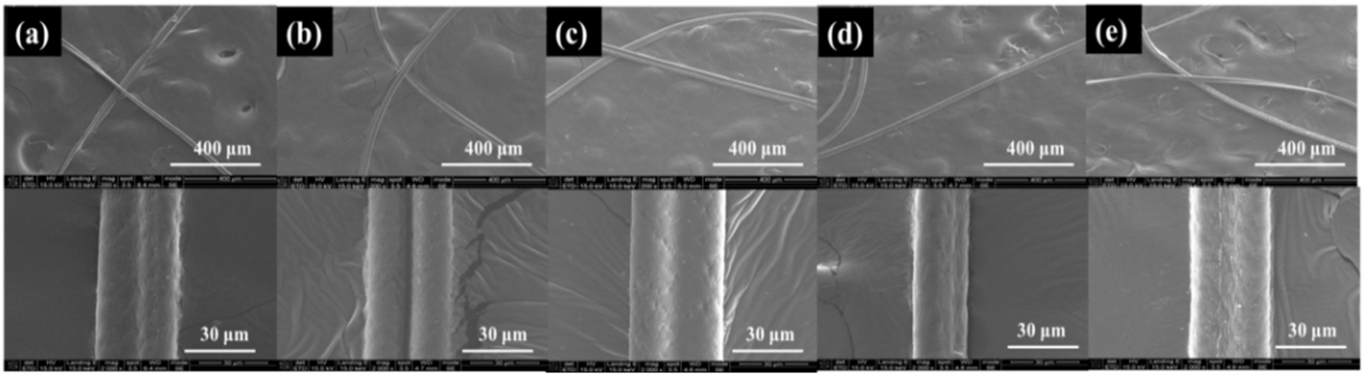

Fig. 4. SEM images of the fibers (a) PANF, (b) PAN$_{PA-2}$F, (c) CuCl$_2$@PAN$_{PA-2}$F, (d) Cu(OAc)$_2$@PAN$_{PA-2}$F and (e) CuSO$_4$@PAN$_{PA-2}$F.

(Fig. 5a). As shown in Fig. 5b, the nanostructured $CuCl_2$ particles was clearly distributed along the fiber.

2.3. Catalytic activity

After comprehensive characterization, the catalytic activity of the fiber-supported copper catalyst was investigated in Chan-Lam coupling. Initially, the reaction of phenylboronic acid with imidazole was chosen as the model to optimize reaction conditions (Table 2). No target product was detected in blank control or in the presence of PANF as the reaction proceeded at 40 °C in CH_3OH for 5 h (**entries 1–2**). When CuCl$_2$@PAN$_{PA-2}$F was used as the catalyst, the coupling reaction proceeded smoothly and the desired product **3a** was obtained in a good yield of 78% (**entry 3**). This result indicates the copper was the genuine catalytic site. Other fiber-supported copper catalysts were then examined and the results showed that Cu(OAc)$_2$@PAN$_{PA-2}$F could afford a moderate yield of **3a** while CuSO$_4$@PAN$_{PA-2}$F displayed inferior activity with a low yield of 24% (**entries 4–5**). In addition to heterogeneous supported-copper catalyst, homogeneous copper salts, such as $CuCl_2 \cdot 2H_2O$, $Cu(OAc)_2 \cdot H_2O$ and $CuSO_4 \cdot 5H_2O$, were employed as catalyst, and the corresponding coupling products were isolated in 67%, 58% and 15% yields after 5 h, respectively (**entries 6–8**). In general, immobilization of a homogeneous catalyst onto solid support would lead to a decrease of activity and selectivity because of the disfavored kinetics of biphasic catalytic system [57]. Apparently, from above results, we can see that the immobilization of diverse copper catalysts onto fiber material gave no detrimental effect on their catalytic performance, and the immobilized catalysts were even slightly better than their homogeneous

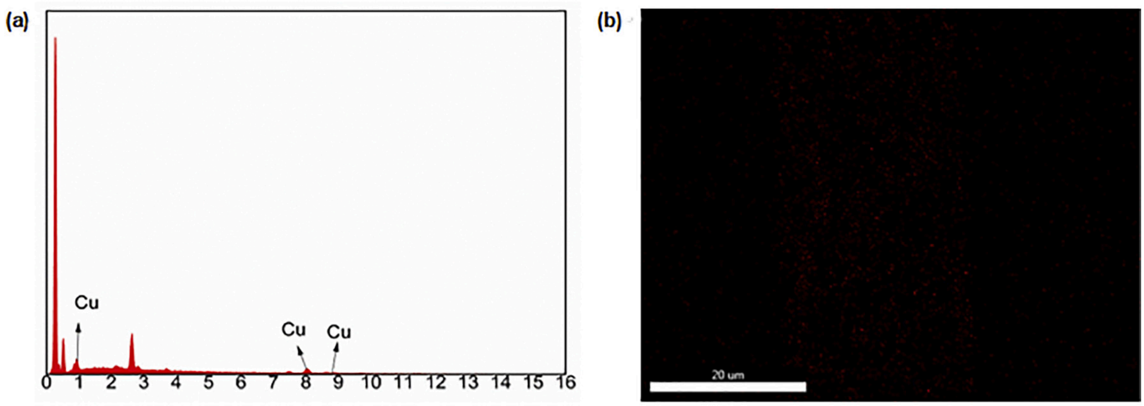

Fig. 5. EDX spectrum (a) and Cu mapping (b) of $CuCl_2$@$PAN_{PA\text{-}2}F$.

counterparts. Considering the convenient separation of catalyst by simple filtration, the fiber supported-catalyst displayed remarkable advantages in the catalytic application. Further studies show that reaction temperature played important impact on the reaction (**entries 9–11**). When the reaction was performed in CH_3OH at an elevated temperature of 60 °C, the yield of **3a** could reach up to 98% within less reaction time in the presence of $CuCl_2$@$PAN_{PA\text{-}2}F$.

It is worth to note that the adjustment of Cu loading of fiber catalyst can significantly influence its catalytic activity. Comparative experiments suggested that lower loading resulted in distinct reduction of catalytic performance as 0.54 mmol g^{-1} $CuCl_2$@$PAN_{PA\text{-}2}F$ only afforded a 65% yield, while the improvement of Cu loading showed better performance as 0.90 mmol g^{-1} $CuCl_2$@$PAN_{PA\text{-}2}F$ gave an excellent yield of 98% under the same conditions (Table 2, **entries 12–14**). The low Cu loading indicates the sparse distribution of catalytic sites upon fiber surface, which resulted in poor accessibility of active sites. In contrast, the higher Cu density probably enhanced the utilization of catalytic sites and hence increased the catalytic efficiency under the same conditions.

Next, we investigated the effect of catalyst dosage, solvent and reactant ratio on model reaction using $CuCl_2$@$PAN_{PA\text{-}2}F$ as optimal catalyst (Table 3). When we changed the catalyst amount from 8 mol% to 5 mol%, the yield of 3a decreased to 84% (**entry 2**). And the use of 2 mol% of $CuCl_2$@$PAN_{PA\text{-}2}F$ only afforded 3a in a 45% yield, whereas

Table 3
Optimization of the other reaction conditions.[a]

Entry	Cat. amount (mol%)	Solvent	Time (h)	Yield (%)[b]
1	8	CH_3OH	3	98
2	5	CH_3OH	3	84
3	2	CH_3OH	6	45
4	10	CH_3OH	3	98
5	8	EtOH	3	47
6	8	H_2O	3	31
7	8	H_2O:CH_3OH (1:1)	3	86
8	8	CH_3CN	3	trace
9	8	EtOAc	3	trace
10	8	CH_2Cl_2	3	trace
11	8	Toluene	3	trace
12[c]	8	CH_3OH	3	93
13[d]	8	CH_3OH	3	98

[a] Reaction conditions: 0.6 mmol phenylboronic acid (1.2 equiv) and 0.5 mmol imidazole (1.0 equiv), 60 °C, solvent (4 mL).
[b] Isolated yield.
[c] 1.1 equiv. of phenylboronic acid was used.
[d] 1.3 equiv. of phenylboronic acid was used.

Table 2
Optimization of fiber catalysts.[a]

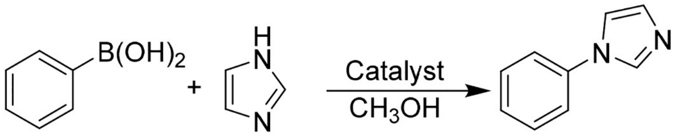

Entry	Catalyst	Temp. (°C)	Time (h)	Yield (%)[b]
1	–	40	5	–
2	PANF	40	5	–
3	$CuCl_2$@$PAN_{PA\text{-}2}F$	40	5	78
4	$Cu(OAc)_2$@$PAN_{PA\text{-}2}F$	40	5	72
5	$CuSO_4$@$PAN_{PA\text{-}2}F$	40	5	24
6	$CuCl_2 \bullet 2H_2O$	40	5	67
7	$Cu(OAc)_2 \bullet H_2O$	40	5	58
8	$CuSO_4 \bullet 5H_2O$	40	5	15
9	$CuCl_2$@$PAN_{PA\text{-}2}F$	50	5	89
10	$CuCl_2$@$PAN_{PA\text{-}2}F$	60	3	98
11	$CuCl_2$@$PAN_{PA\text{-}2}F$	reflux	3	98
12[c]	$CuCl_2$@$PAN_{PA\text{-}2}F$	60	3	65
13[d]	$CuCl_2$@$PAN_{PA\text{-}2}F$	60	3	84
14[e]	$CuCl_2$@$PAN_{PA\text{-}2}F$	60	3	98

[a] Reaction conditions: phenylboronic acid (0.6 mmol) and imidazole (0.5 mmol), catalyst (8 mol%), solvent (4 mL); [b] Isolated yield; [c,d,e] The Cu loading of $CuCl_2$@$PAN_{PA\text{-}2}F$ is 0.54, 0.68 and 1.07 mmol g^{-1}, respectively.

Table 4

Chan-Lam coupling reaction of arylboronic acids with different 1*H*-imidazole nucleophiles.[a]

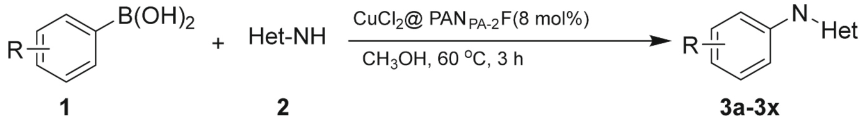

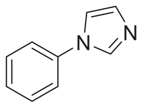

3a, 98%

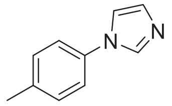

3b, 97%

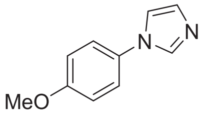

3c, 94%

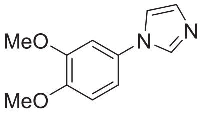

3d, 95%

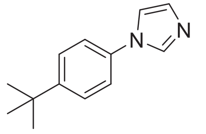

3e, 95%

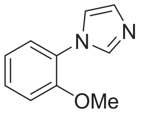

3f, 86%

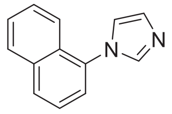

3g, 93%

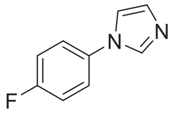

3h, 85%

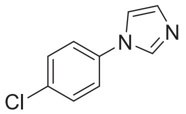

3i, 87%

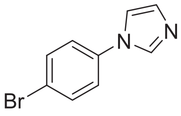

3j, 88%

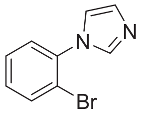

3k, 80%

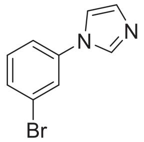

3l, 83%

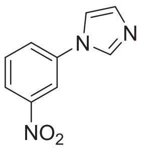

3m, 79%

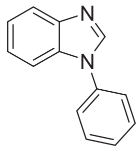

3n, 96%

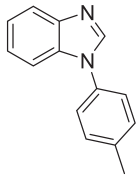

3o, 95%

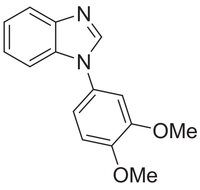

3p, 93%

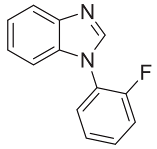

3q, 81%

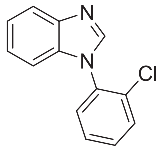

3r, 83%

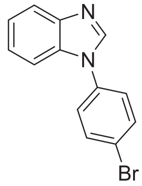

3s, 85%

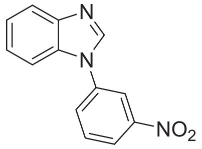

3t, 72%

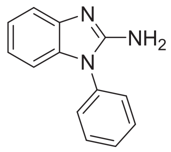

3u, 89%

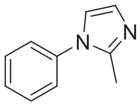

3v, 93%

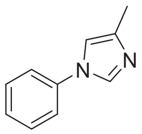

3w, 89%

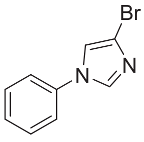

3x, 85%

[a] Reaction conditions: **1** (0.6 mmol) and **2** (0.5 mmol), $CuCl_2$@$PAN_{PA\text{-}2}F$ (8 mol%), CH_3OH (4 mL), 60 °C, 3 h.

additional catalyst amount gave no improvement of yield (**entries 3–4**). Hence, the catalyst dosage of 8 mol% was necessary for the coupling reaction toward completion (**entry 1**). Among the solvents tested, it was found that other polar proton solvents, ethanol and water, were not beneficial to this reaction and resulted in the formation of **3a** in lower yields of 47% and 31%, respectively (**entries 5–6**). The use of a mixture solvent of methanol and water provided a good yield and was better than that in water (**entry 7**). This result indicates that fiber catalyst system could perform well in aqueous media but methanol was more preferred. Other solvents, such as CH_3CN, EtOAc, CH_2Cl_2, toluene, and *n*-hexane gave only trace of product (**entries 8–11**). The phenomena were presumably due to the good solubility of reactants in these solvents failed to make them enriched into the surface microenvironment of the fiber catalyst and effectively contacting with the catalytic sites. Using methanol as the solvent, good enrichment of the reactants into the fiber surface was provided. In addition, it was observed that the fiber catalyst spread better in methanol than in ethanol, which indicates the accessibility of catalytic sites in fiber surface was more efficient in methanol. Furthermore, when the reaction was performed with a 1:1 M ratio of two coupling partners, desired product was obtained in 93% yield (**entry 12**). Increasing the amount of phenylboronic acid could improve the product yield and 1.2 equiv. of boronic acid was found to be the optimal amount (**entries 1 and 13**).

With the optimal conditions in hand, a variety of structurally diverse substrates were tested to explore generality of this catalytic system and the results are shown in Table 4. We are glad to observe that the reactions of various substituted arylboronic acids with imidazole proceed smoothly and the corresponding *N*-arylimidazoles were obtained in good to excellent yields. Arylboronic acids with electron-donating alkyl and alkoxy groups at para or meta position gave desired products **3b-3f** in high yields ranging from 94 to 97%, while ortho-substituted methoxy group **3f** provided relatively lower yield which was possibly attributed to larger steric hindrance. Halogen-substituted phenylboronic acids (fluoro, chloro and bromo) proved effective coupling partners and their corresponding products were isolated in 80–88% yields, whereas strong electron-withdrawing nitro-substituted phenylboronic acid gave a low yield of product **3m**. It was observed that phenylboronic acid, *p*-tolyboronic acid, and 3,4-dimethoxyphenylboronic acid were favorably converted to the corresponding *N*-arylbenzimidazoles when benzimidazole was used as a nucleophile. The presence of electron-withdrawing halogen groups in the benzene ring was also well tolerated. Moreover, the reaction between phenylboronic acid and *N*1-arylated 2-aminobenzimidazole **3u** in an 89% yield. To further extend the substrate scope, other substituted imidazoles (2-methyl-1*H*-imidazole, 4-methyl-1*H*-imidazole and 4-bromo-1*H*-imidazole) have been tried in the reaction, and the coupling products **3v-3x** were generated in 93%, 89% and 85% yields, respectively.

Based on the high-efficiency of $CuCl_2$@$PAN_{PA\text{-}2}F$ in Chan-Lam coupling for the synthesis of *N*-arylimidazoles, we further explored the utility of the fiber catalyst in the synthesis of *N*-arylsulfonamides. The coupling reaction of phenylboronic acid with tosyl azide was chosen as the model. As show in Table S2, $CuCl_2$@$PAN_{PA\text{-}2}F$ was proved to be effective in the reaction, and the desired product was obtained in a 91% yield after 0.5 h at 60 °C (**entry 1**). Under catalyst-free conditions, only a trace amount of product was generated. Also, PANF itself was found to be inactive in the reaction (**entries 2–3**). The effect of solvent on the reaction was studied and it was found that no case showed superiority to CH_3OH (**entries 6–9**). Reducing the catalyst dosage or reactant ratio of phenylboronic acid to tosyl azide caused the obvious decline of yield (**entries 5** and **10**). Regarding the reaction temperature, a lower temperature of 40 °C offered the product in a 45% yield (**entry 11**). According to above results, the optimal conditions were confirmed as follows: $CuCl_2$@$PAN_{PA\text{-}2}F$ (5 mol%), CH_3OH, 60 °C, 0.5 h. With the optimized conditions in hand, the generality of fiber catalyst in the coupling reaction of arylboronic acids with tosyl azide was evaluated and the results are shown in Table 5. It can be seen that arylboronic acids bearing either electron-donating or electron-withdrawing group smoothly reacted with tosyl azide to give the corresponding products in high yields (83–94%).

In addition, gram-scale synthesis of *N*-arylimidazole and *N*-arylsulfonamides was conducted. As show in Scheme 2, the reactions with 10 mmol scale underwent effectively and the desired *N*-arylated products **3a** and **5a** were obtained in stationary yields without any elevation of reaction temperature or extension of reaction time, suggesting the potential application of this fiber-mediated catalytic system in large-scale production.

2.4. Recycling and leaching experiments

One of the most important features of heterogeneous catalyst is the recyclability, namely, the supported-catalyst can be easily separated from reaction system for multiple reuse. To verify the recyclability of $CuCl_2$@$PAN_{PA\text{-}2}F$, the model coupling reaction of phenylboronic acid with imidazole was conducted under optimized conditions. After completion of the reaction, the fiber catalyst was separated by filtration and washed with ethylacetate to remove the absorbed product before next run. The result showed that the reaction yields of the first to the fifth runs were 98%, 96%, 91%, 84% and 78%, respectively, indicating $CuCl_2$@$PAN_{PA\text{-}2}F$ could be reused five times with high activity. The recovered fibers were subsequently examined by mechanical strength test and SEM. The breaking strength of $CuCl_2$-5@$PAN_{PA\text{-}2}F$ was only 0.29 cN lower than that of fresh $CuCl_2$@$PAN_{PA\text{-}2}F$, that is, 96% of strength was maintained (Table S3, **entry 2**). Meanwhile, there was no obvious collapse or fracture in the surface of $CuCl_2$-5@$PAN_{PA\text{-}2}F$, albeit wrinkled and rough (Fig. S2). These observations suggested that the structure of fiber catalyst was not obviously destroyed after multiple reuse.

Leaching experiment was then carried out to ascertain whether $CuCl_2$@$PAN_{PA\text{-}2}F$ mediated heterogeneous catalytic process (Table S4). When the coupling reaction of phenylboronic acid with imidazole proceeded for 2 h under the optimized conditions, fiber catalyst was taken out quickly from the system, and the residue mixture was stirred for another 1 h. The result showed that the reaction of remaining reaction mixture almost gave no additional yield, which means the leaching $CuCl_2$ catalyst had very low activity, and the heterogeneous nature of fiber catalytic system was confirmed. In order to evaluate the Cu leaching, atomic absorption spectroscopy (AAS) was conducted for the reaction mixtures after the recycled $CuCl_2$@$PAN_{PA\text{-}2}F$ was removed from first to fourth run. The ratios of leaching Cu into the methanol were found to be 72.0%, 7.5%, 3.4% and 0.5%, respectively, and AAS analysis of the recycled catalyst after fourth run showed 12.4% of initial Cu was kept in the catalyst. The remaining ratios of Cu (28.0%, 20.5%, 17.1%, 16.6%) did not well match the corresponding yields from second to fifth runs in the above reuse experiments, which further supported that the chelated Cu ions in the relatively hydrophobic microenvironment of fiber surface were the major catalytic sites.

Table 5
Chan-Lam coupling reaction of arylboronic acid with tosyl azide.[a,b]

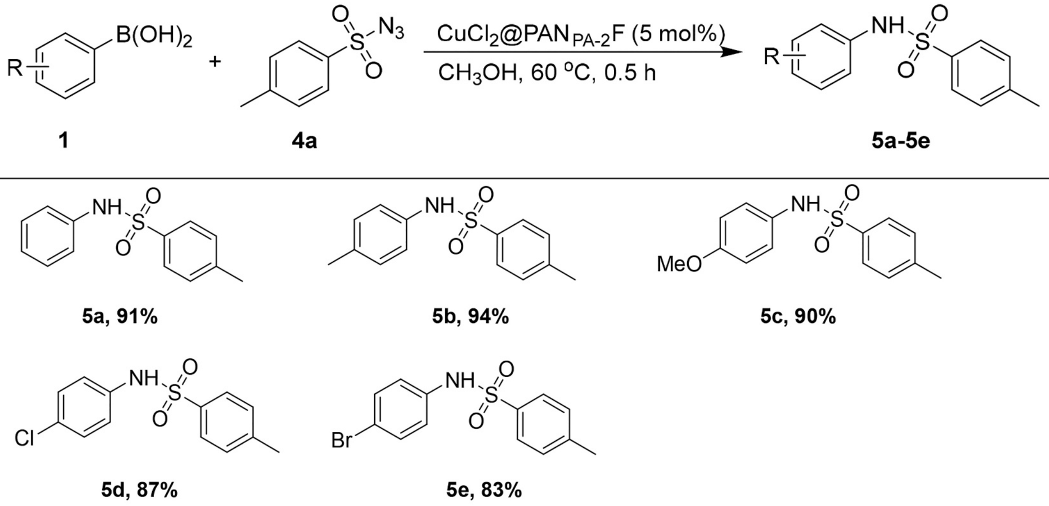

[a] Reaction conditions: **1** (0.6 mmol) and **4a** (0.5 mmol), $CuCl_2$@$PAN_{PA\text{-}2}F$ (5 mol%), CH_3OH (4 mL), 60 °C, 0.5 h. [b] All yields are isolated yield.

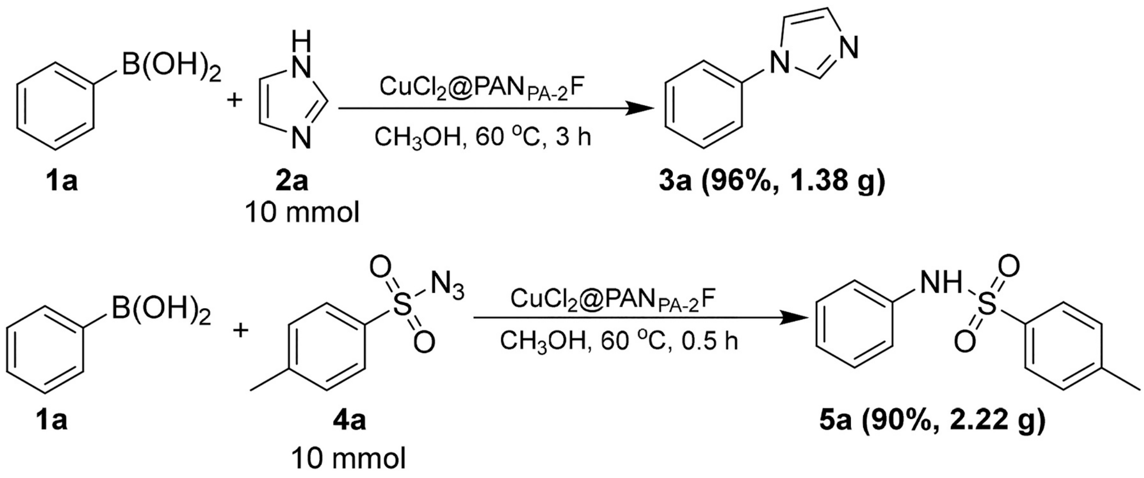

Scheme 2. Gram-scale reaction.

Table 6
Comparison of different catalytic system in Chan-Lam coupling reaction for the synthesis of *N*-phenylimidazole[a].

Entry	Catalyst	Reaction conditions	Yield (%)	Run	Ref
1	SiO_2-NHC-Cu	MeOH, 50 °C, 3 h	90	6	[58]
2	PS-Cu	MeOH, 40 °C, 10 h	99	5	[31]
3	Cu@PI-COF	MeOH-H_2O, rt., 8 h	87	8	[17]
4	Cu-(tpa) MOF	EtOH, Et_3N, rt., 12 h	99	5	[32]
5	$Cu_3(BTC)_2$	EtOH, Et_3N,60 °C, 12 h	92	4	[33]
6	Cu-doped $CoFe_2O_4$	MeOH, Et_3N, rt., 5 h	92	7	[59]
7	URJC-1-MOF	DMF, K(OAc), rt., 15 h	61	5	[60]
8	CuO NPs	MeOH-H_2O, K_2CO_3, rt., 10 h	88	6	[61]
9	$Cu_{30}I_{16}(mtpmt)_{12}(\mu_{10}\text{-}S_4)$	MeOH, Et_3N, rt., 5 h	99	5	[62]
10	$CuCl_2$@$PAN_{PA\text{-}2}F$	MeOH, 60 °C, 3 h	98	5	This work

[a] Chan-Lam coupling of benzalboronic acid and imidazole as template reaction.

2.5. Comparison of different catalytic systems in Chan-Lam coupling toward N-phenylimidazole

In order to evaluate the efficiency of present fiber catalyst, we compared the obtained results with those of previously reported heterogeneous catalysts (Table 6). Although the coupling worked well at room temperature, additional bases and prolonged reaction time were generally required (**entries 4–9**). Fiber-supported catalyst has comparable catalytic activity with these commonly silica and MOF supported catalysts without any base at an elevated temperature in short reaction time. More importantly, the fiber catalyst exhibited the advantage of easier separation by filtration over these particle catalysts because of the regular and flexible structure of fiber.

2.6. Reaction mechanism

Since Chan-Lam couplings of arylboronic acid with amine/imidazole were reported, different reaction mechanisms have been proposed [27]. Recently, Cu(III) species has been increasingly favored as the intermidiate, which is generated through oxidation with O_2 or possible disproportionaliztion. Since the coupling of phenylboronic acid with imidazole catalyzed by $CuCl_2$@$PAN_{PA\text{-}2}F$ in N_2 atmosphere under the standard conditions only gave trace amount of product, Cu(III)-based mechanism is preferred for this trnasformation. Although the chelated $CuCl_2$ is the minor component of the fiber catalyst, it is possibly the more active site, whereas $CuCl_2$ particles traped and wraped in fiber surface are more likely the resevior of copper ions than major active sites, because the copper complexes with ligands were commonly more active than the corresponding copper salts in literatures, and the bulky $CuCl_2$ particles had limited surface area to catalyze the reaction efficiently. According to the related mechanisms proposed in literatures [22,25,27,32] and our observations, plausible mechanism of $CuCl_2$@$PAN_{PA\text{-}2}F$ catalyzed reaction of arylboronic acid and imidazole is proposed as shown in Scheme 3.

As the fiber surface contains excess basic prolinamide moiety, arylboronic acid was more easily to access the prolinamide moiety, thus the transmetalation of arylboronic acid with the fiber catalyst was more accepted as the first step than that of imidazole with catalyst proposed very recently [63]. The formed intermediate **A** was coordinated with imidazole to generate intermediate **B**, which was oxidized by O_2 to Cu (III) species **C**. In this aerobic oxidation process, the generated water would react with $ClB(OH)_3$ to form $B(OH)_3$ and HCl. The free prolinamide moiety adjacent to the chelated Cu(II) could also promote this process cooperatively by combining with HCl. The reductive elimination of **C** yielded the coupling product *N*-arylimidazole and Cu(I) species **D**. The following aerobic oxidation step could make the Cu(II) catalyst recovered in the aid of released HCl from prolinamide moiety.

3. Conclusion

In summary, we have described an efficient, stable and recyclable fiber-immobilized copper catalyst in Chan-Lam coupling for the production of *N*-arylimidazole and *N*-arylsulfonamides. The fiber catalysts were readily prepared by the incorporation of prolinamide unit into PANF and the subsequent immobilization of copper(II) in aqueous solution. Cu(II) ions mainly gathered in the microenvironment of fiber surface as particles and form an equilibrium with chelated Cu(II) ions, although the latter was thought as the major catalytic sites. Excellent physical and chemical stability of fiber catalysts were demonstrated by mechanical strength test, thermal analysis and solvent resistance experiments. Among the prepared catalysts, $CuCl_2$@$PAN_{PA\text{-}2}F$ exhibited the best catalytic performance in the coupling of arylboronic acids with imidazole as well as tosyl azide, giving desired products in good to excellent yields. The catalytic activity of fiber catalyst was improved by adjusting the Cu loading. Further studies show that $CuCl_2$@$PAN_{PA\text{-}2}F$ could be simply recovered by filtration, recycled for five times, and perform well in gram-scale experiments. This fiber-mediated catalytic

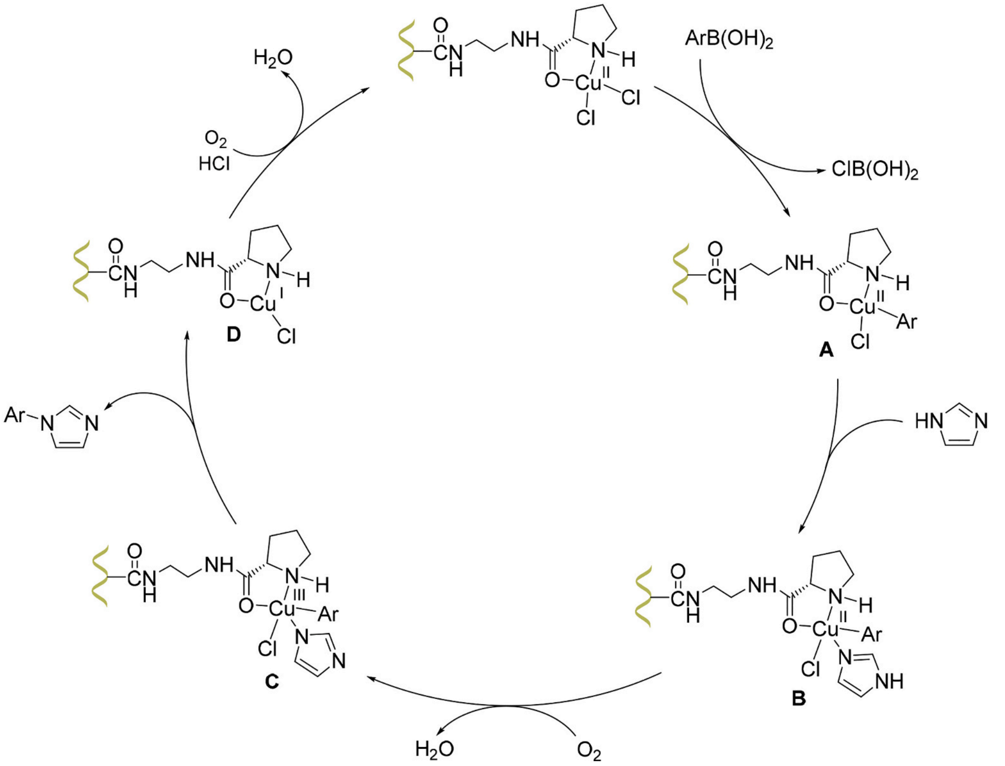

Scheme 3. Proposed mechanism of Chan-Lam coupling reaction between phenylboronic acid and imidazole by fiber-supported copper catalyst.

system is efficient, convenient and sustainable with possible application in large-scale production. Moreover, the plausible mechanism for the $CuCl_2$@$PAN_{PA\text{-}2}F$-catalyzed coupling of arylboronic acid with imidazole has been proposed.

4. Experimental section

4.1. Materials and reagents

Commerically PANF (length of 10 cm and a diameter of 30 ± 0.5 μm) with the composition of 93% acrylonitrile, 6.5% methyl acrylate, and 0.4–0.5% sodium styrene sulfonate were purchased from Fushun Petrochemical Corporation of China. L-proline methyl ester hydrochloride, triethylamine, ethane-1,2-diamine, $CuCl_2\cdot 2H_2O$, $Cu(OAc)_2\cdot H_2O$, $CuSO_4\cdot 5H_2O$, phenylboronic acid, imidazole, benzimidazole, tert-butyl methyl ether, dichloromethane, methanol, petroleum ether, ethyl acetate, and other reagents were analytical grade and used without further purification.

4.2. Instruments

The Fourier transform infrared spectra (FT-IR) of fiber was recorded using AVATAR360 FT-IR spectrometer (Thermo Nicolet). The sample of fiber was cut to pieces and compressed into KBr pellets before measurement. X-ray power diffraction (XRD) of fiber was carried out with D/MAX-2500 X-ray diffractometer (Rigaku Corporation). Thermostability of fiber was measured using STA409PC TGA/DSC simultaneous thermalanalyzer (Netzsch Company, Germany). Elemental analysis was performed on Vario Micro Cube instrument (Elementar, Germany). Surface morphology of fiber was determined using scanning electron microcopy (Hitachi, model S-4800). XPS was performed on Thermo ESCALAB 250XI spectrometer (ThermoFisher Scientific, America). AAS (atomic absorption spectrometry) was carried out using Ice3300. NMR spectra of products (^1H for 400 MHz and ^{13}C for 101 MHz) were recorded on BRUKER-AVANCE III instruments in $CDCl_3$ with TMS as internal standard.

4.3. Preparation of prolinamide-functionalized fiber $PAN_{PA\text{-}2}F$

Dried PANF (0.47 g) was added to a solution of (*S*)-*N*-(2-aminoethyl) pyrrolidine-2-carboxamide (5.00 g) dissolved in ethylene glycol (6.5 mL) in a round-bottom flask, followed by stirring at 140 °C for 3 h. After being cooled to room temperature, the fiber was taken out using tweezers, washed with deionized water, and dried at 60 °C for 12 h to give prolinamide-fiber $PAN_{PA\text{-}2}F$ (1.15 mmol g^{-1}). Other modification degree of prolinamide-fiber was gained by reducing the reaction time (0.74 mmol g^{-1} for 1.5 h; 0.93 mmol g^{-1} for 2 h). Additionally, when above mixture was stirred at 150 °C for 3 h, a higher modification degree of $PAN_{PA\text{-}2}F$ (1.39 mmol g^{-1}) was obtained.

4.4. Preparation of $CuCl_2$@$PAN_{PA\text{-}2}F$

Dried $PAN_{PA\text{-}2}F$ (0.5 g) was added to an aqueous solution of cupric chloride (0.5 mol L^{-1}, 15 mL) and the mixture was stirred at room temperature for 24 h. After that, the fiber was collected by filtration, washed with ethanol (200 mL) and water (200 mL), and dried at 60 °C for 12 h under vacuum to give fiber-supported copper catalyst $CuCl_2$@$PAN_{PA\text{-}2}F$.

4.5. Preparation of $Cu(OAc)_2$@$PAN_{PA\text{-}2}F$ and $CuSO_4$@$PAN_{PA\text{-}2}F$

The preparation of $Cu(OAc)_2$@$PAN_{PA\text{-}2}F$ and $CuSO_4$@$PAN_{PA\text{-}2}F$ are similar to that of $CuCl_2$@$PAN_{PA\text{-}2}F$. Typically, $Cu(OAc)_2$@$PAN_{PA\text{-}2}F$ was prepared from $PAN_{PA\text{-}2}F$ (0.536 g) with the aqueous solution of cupric acetate (0.5 mol L^{-1}, 15 mL) at room temperature for 24 h, and $CuSO_4$@$PAN_{PA\text{-}2}F$ was prepared from $PAN_{PA\text{-}2}F$ with the aqueous solution of cupric sulfate (0.5 mol L^{-1}, 15 mL) at room temperature for 24 h.

Declaration of Competing Interest

There are no conflicts of interest to declare.

Acknowledgements

This work was financially supported by the National Natural Science Foundation of China (No. 21777111).

Appendix A. Supplementary data

Supplementary data to this article can be found online at https://doi.org/10.1016/j.reactfunctpolym.2021.104831.

References

[1] J. Bariwal, E. van der Eycken, C-N bond forming cross-coupling reactions: an overview, Chem. Soc. Rev. 42 (2013) 9283–9303.

[2] Q. Wang, Y. Su, L. Li, H. Huang, Transition-metal catalysed C-N bond activation, Chem. Soc. Rev. 45 (2016) 1257–1272.

[3] W. Guo, M. Zhao, W. Tan, L. Zheng, K. Tao, X. Fan, Developments towards synthesis of N-heterocycles from amidines via C–N/C–C bond formation, Org. Chem. Front. 6 (2019) 2120–2141.

[4] S.A. Laufer, W. Zimmermann, K.J. Ruff, Tetrasubstituted imidazole inhibitors of cytokine release: probing substituents in the *N*-1 position, J. Med. Chem. 47 (2004) 6311–6325.

[5] R.A. Fromtling, Overview of medically important antifungal azole derivatives, Clin. Microbiol. Rev. 1 (1988) 187–217.

[6] T.R. Shape, S.C. Cherkofsky, W.E. Hewes, D.H. Smith, W.A. Gregory, S.B. Haber, Preparation and antiarthritic and analgesic activity of 4,5-diaryl-2-(substituted thio)-iff-imidazoles and their sulfoxides and sulfones, J. Med. Chem. 28 (1998) 1188–1194.

[7] J. Dupont, R.F. de Souza, P.A. Suarez, Ionic liquid (molten salt) phase organometallic catalysis, Chem. Rev. 102 (2002) 3667–3692.

[8] J.P. Hallett, T. Welton, Room-temperature ionic liquids: solvents for synthesis and catalysis. 2, Chem. Rev. 111 (2011) 3508–3576.

[9] J.C. Lin, R.T. Huang, C.S. Lee, A. Bhattacharyya, W.S. Hwang, I.J. Lin, Coinage metal-*N*-heterocyclic carbene complexes, Chem. Rev. 109 (2009) 3561–3598.

[10] M.N. Hopkinson, C. Richter, M. Schedler, F. Glorius, An overview of *N*-heterocyclic carbenes, Nature 510 (2014) 485–496.

[11] T. Schulz, C. Torborg, B. Schaffner, J. Huang, A. Zapf, R. Kadyrov, A. Borner, M. Beller, Practical imidazole-based phosphine ligands for selective palladium-catalyzed hydroxylation of aryl halides, Angew. Chem. Int. Ed. 48 (2009) 918–921.

[12] E.B. Anderson, T.E. Long, Imidazole- and imidazolium-containing polymers for biology and material science applications, Polymer 51 (2010) 2447–2454.

[13] J. Pina, J.S. Seixas de Melo, R.M. Batista, S.P. Costa, M.M. Raposo, Synthesis and characterization of the ground and excited states of tripodal-like oligothienyl-imidazoles, J. Phys. Chem. B 114 (2010) 4964–4972.

[14] J. Ohmori, M. Shimizu-Sasamata, M. Okada, S. Sakamoto, Novel AMPA receptor antagonists: synthesis and structure-activity relationships of 1-hydroxy-7-(1H-imidazol-1-yl)-6-nitro-2,3(1H,4H)-quinoxalinedione and related compounds, J. Med. Chem. 39 (1996) 3971–3979.

[15] A. Klapars, J.C. Antilla, X. Huang, S.L. Buchwald, A general and efficient copper catalyst for the amidation of aryl halides and the N-arylation of nitrogen heterocycles, J. Am. Chem. Soc. 123 (2001) 7727–7729.

[16] J. Hassan, M. Sevignon, C. Gozzi, E. Schulz, M. Lemaire, Aryl-aryl bond formation one century after the discovery of the Ullmann reaction, Chem. Rev. 102 (2002) 1359–1470.

[17] R.A. Altman, E.D. Koval, S.L. Buchwald, Copper-catalyzed *N*-arylation of imidazoles and benzimidazoles, J. Org. Chem. 72 (2007) 6190–6199.

[18] P. Suresh, K. Pitchumani, Per-6-amino-beta-cyclodextrin as an efficient supramolecular ligand and host for Cu(I)-catalyzed N-arylation of imidazole with aryl bromides, J. Org. Chem. 73 (2008) 9121–9124.

[19] C. Sambiagio, S.P. Marsden, A.J. Blacker, P.C. McGowan, Copper catalysed Ullmann type chemistry: from mechanistic aspects to modern development, Chem. Soc. Rev. 43 (2014) 3525–3550.

[20] D.M.T. Chan, K.L. Monaco, R.P. Wang, M.P. Winters, New N- and O-arylations with phenylboronic acids and cupric acetate, Tetrahedron Lett. 39 (1998) 2933–2936.

[21] P.Y.S. Lam, C.G. Clark, S. Saubern, J. Adams, M.P. Winters, D.M.T. Chan, A. Combs, New aryl/heteroaryl C-N bond cross-coupling reactions via arylboronic acid cupric acetate arylation, Tetrahedron Lett. 39 (1998) 2941–2944.

[22] J.P. Collman, M. Zhong, An efficient diamine.copper complex-catalyzed coupling of arylboronic acids with imidazoles, Org. Lett. 2 (2000) 1233–1236.

[23] J.C. Antilla, J.M. Baskin, T.E. Barder, S.L. Buchwald, Copper-diamine-catalyzed N-arylation of pyrroles, pyrazoles, indazoles, imidazoles, and triazoles, J. Org. Chem. 69 (2004) 5578–5587.

[24] J. Qiao, P. Lam, Copper-promoted carbon-heteroatom bond cross-coupling with boronic acids and derivatives, Synthesis 2011 (2010) 829–856.

[25] D.N. Rao, S. Rasheed, R.A. Vishwakarma, P. Das, Copper-catalyzed sequential *N*-arylation of C-amino-NH-azoles, Chem. Commun. 50 (2014) 12911–12914.

[26] X. Jia, P. Peng, N,O-Bidentate ligand-tunable copper(II) complexes as a catalyst for Chan-Lam coupling reactions of arylboronic acids with 1*H*-imidazole derivatives, Org. Biomol. Chem. 16 (2018) 8984–8988.

[27] M.J. West, J.W.B. Fyfe, J.C. Vantourout, A.J.B. Watson, Mechanistic development and recent applications of the chan-lam amination, Chem. Rev. 119 (2019) 12491–12523.

[28] P.R. Likhar, S. Roy, M. Roy, M.L. Kantam, R.L. De, Silica immobilized copper complexes: efficient and reusable catalysts for N-arylation of *N*(H)-heterocycles and benzyl amines with aryl halides and arylboronic acids, J. Mol. Catal. A 271 (2007) 57–62.

[29] Y.L. Cui, X.N. Guo, Y.Y. Wang, X.Y. Guo, Visible-light-driven photocatalytic *N*-arylation of imidazole derivatives and arylboronic acids on Cu/graphene catalyst, Sci. Rep. 5 (2015) 12005.

[30] S.M. Islam, S. Mondal, P. Mondal, A.S. Roy, K. Tuhina, N. Salam, M. Mobarak, A reusable polymer supported copper catalyst for the C-N and C-O bond cross-coupling reaction of aryl halides as well as arylboronic acids, J. Organomet. Chem. 696 (2012) 4264–4274.

[31] S.M. Islam, N. Salam, P. Mondal, A.S. Roy, K. Ghosh, K. Tuhina, A highly active reusable polymer anchored copper catalyst for C-O, C-N and C-S cross coupling reactions, J. Mol. Catal. A 387 (2014) 7–19.

[32] N. Devarajan, P. Suresh, Framework-copper-catalyzed C−N cross-coupling of arylboronic acids with imidazole: convenient and ligand-free synthesis of *N*-Arylimidazoles, ChemCatChem 8 (2016) 2953–2960.

[33] N. Anbu, A. Dhakshinamoorthy, Cu$_3$(BTC)$_2$ metal-organic framework catalyzed *N*-arylation of benzimidazoles and imidazoles with phenylboronic acid, J. Ind. Eng. Chem. 65 (2018) 120–126.

[34] Y. Han, M. Zhang, Y.-Q. Zhang, Z.-H. Zhang, Copper immobilized at a covalent organic framework: an efficient and recyclable heterogeneous catalyst for the Chan–Lam coupling reaction of aryl boronic acids and amines, Green Chem. 20 (2018) 4891–4900.

[35] H. Sharma, H. Mahajan, B. Jamwal, S. Paul, Cu@Fe$_3$O$_4$-TiO$_2$-L-dopa: a novel and magnetic catalyst for the Chan-Lam cross-coupling reaction in ligand free conditions, Catal. Commun. 107 (2018) 68–73.

[36] R. Zhao, X. Li, B. Sun, Y. Li, Y. Li, R. Yang, C. Wang, Branched polyethylenimine grafted electrospun polyacrylonitrile fiber membrane: a novel and effective adsorbent for Cr(VI) remediation in wastewater, J. Mater. Chem. A 5 (2017) 1133–1144.

[37] S. Deng, R.B. Bai, Aminated polyacrylonitrile fibers for humic acid adsorption: behaviors and mechanisms, Environ. Sci. Technol. 37 (2003) 5799–5805.

[38] Y. Fan, H.J. Liu, Y. Zhang, Y. Chen, Adsorption of anionic MO or cationic MB from MO/MB mixture using polyacrylonitrile fiber hydrothermally treated with hyperbranched polyethylenimine, J. Hazard. Mater. 283 (2015) 321–328.

[39] X. Li, C. Zhang, R. Zhao, X. Lu, X. Xu, X. Jia, C. Wang, L. Li, Efficient adsorption of gold ions from aqueous systems with thioamide-group chelating nanofiber membranes, Chem. Eng. J. 229 (2013) 420–428.

[40] G. Xu, L. Wang, M. Li, M. Tao, W. Zhang, Phosphorous acid functionalized polyacrylonitrile fibers with a polarity tunable surface micro-environment for one-pot C–C and C–N bond formation reactions, Green Chem. 19 (2017) 5818–5830.

[41] G. Li, J. Xiao, W. Zhang, Knoevenagel condensation catalyzed by a tertiary-amine functionalized polyacrylonitrile fiber, Green Chem. 13 (2011) 1828–1836.

[42] J.W. Lee, T. Mayer-Gall, K. Opwis, C.E. Song, J.S. Gutmann, B. List, Organotextile catalysis, Science 341 (2013) 1225–1229.

[43] L. Shao, C. Qi, Preoxidated polyacrylonitrile fiber mats supported copper catalyst for Mizoroki–Heck cross-coupling reactions, Appl. Catal. A Gen. 468 (2013) 26–31.

[44] J. Cao, G. Xu, P. Li, M. Tao, W. Zhang, Polyacrylonitrile fiber supported *N*-heterocyclic carbene Ag(I) as efficient catalysts for three-component coupling and intramolecular 1,3-dipolar cycloaddition reactions under flow conditions, ACS Sustain. Chem. Eng. 5 (2017) 3438–3447.

[45] P. Prasanna, S. Perumal, J.C. Menéndez, Chemodivergent, multicomponent domino reactions in aqueous media: l-proline-catalyzed assembly of densely functionalized 4H-pyrano[2,3-c]pyrazoles and bispyrazolyl propanoates from simple, acyclic starting materials, Green Chem. 15 (2013) 1292–1299.

[46] M. Tsujii, M. Sonoda, S. Tanimori, Proline-mediated transition metal-free access to 1H-indazolones from 2-halobenzohydrazides, J. Org. Chem. 81 (2016) 6766–6773.

[47] B.S. Vachan, M. Karuppasamy, P. Vinoth, S. Vivek Kumar, S. Perumal, V. Sridharan, J.C. Menéndez, Proline and its derivatives as organocatalysts for multicomponent reactions in aqueous media: synergic pathways to the green synthesis of heterocycles, Adv. Synth. Catal. 362 (2019) 87–110.

[48] D. Ma, Q. Cai, Copper/amino acid catalyzed cross-couplings of aryl and vinyl halides with nucleophiles, Acc. Chem. Res. 41 (2008) 1450–1460.

[49] D. Ma, Q. Geng, H. Zhang, Y. Jiang, Assembly of substituted phenothiazines by a sequentially controlled CuI/ L-proline-catalyzed cascade C-S and C-N bond formation, Angew. Chem. Int. Ed. 49 (2010) 1291–1294.

[50] G. Chouhan, D. Wang, H. Alper, Magnetic nanoparticle-supported proline as a recyclable and recoverable ligand for the CuI catalyzed arylation of nitrogen nucleophiles, Chem. Commun. (2007) 4809–4811.

[51] W. Chen, Y. Zhang, L. Zhu, J. Lan, R. Xie, J. You, A concept of supported amino acid ionic liquids and their application in metal scavenging and heterogeneous catalysis, J. Am. Chem. Soc. 129 (2007) 13879–13886.

[52] E. Verde-Sesto, M. Pintado-Sierra, A. Corma, E.M. Maya, J.G. de la Campa, M. Iglesias, F. Sanchez, First pre-functionalised polymeric aromatic framework from mononitrotetrakis(iodophenyl)methane and its applications, Chem. Eur. J. 20 (2014) 5111–5120.

[53] H. Zhu, G. Xu, H. Du, C. Zhang, N. Ma, W. Zhang, Prolinamide functionalized polyacrylonitrile fiber with tunable linker length and surface microenvironment as

efficient catalyst for Knoevenagel condensation and related multicomponent tandem reactions, J. Catal. 374 (2019) 217–229.

[54] X.-L. Shi, Q. Hu, F. Wang, W. Zhang, P. Duan, Application of the polyacrylonitrile fiber as a novel support for polymer-supported copper catalysts in terminal alkyne homocoupling reactions, J. Catal. 337 (2016) 233–239.

[55] L. Fang, S. Dong, L. Shi, Q. Sun, Modification of $CuCl_2{\cdot}2H_2O$ by dielectric barrier discharge and its application in the hydroxylation of benzene, New J. Chem. 43 (2019) 12744–12753.

[56] Y. Yuan, W. Cao, W. Weng, $CuCl_2$ immobilized on amino-functionalized MCM-41 and MCM-48 and their catalytic performance toward the vapor-phase oxy-carbonylation of methanol to dimethylcarbonate, J. Catal. 228 (2004) 311–320.

[57] A.F. Trindade, P.M. Gois, C.A. Afonso, Recyclable stereoselective catalysts, Chem. Rev. 109 (2009) 418–514.

[58] P. Liu, P. Li, L. Wang, SiO_2-NHC-CuI–catalyzed *N*-arylation of imidazoles with arylboronic acids under base-free reaction conditions, Synth. Commun. 42 (2012) 2595–2605.

[59] M.M. Dutta, P. Phukan, Cu-doped $CoFe_2O_4$ nanoparticles as magnetically recoverable catalyst for C-N cross-coupling reaction, Catal. Commun. 109 (2018) 38–42.

[60] A. Muñoz, P. Leo, G. Orcajo, F. Martínez, G. Calleja, URJC-1-MOF as new heterogeneous recyclable catalyst for C-heteroatom coupling reactions, ChemCatChem 11 (2019) 3376–3380.

[61] A. Thakur, R. Borah, P. Raul, A. Mahanta, A. Shchukarev, J.-P. Mikkola, Copper oxide nanoparticles as a mild and efficient catalyst for *N*-arylation of imidazole and aniline with boronic acids at room temperature, Synlett 28 (2017) 1177–1182.

[62] H.X. Li, W. Zhao, H.Y. Li, Z.L. Xu, W.X. Wang, J.P. Lang, $[Cu_{30}I_{16}(mtpmt)_{12}(\mu_{10}\text{-}S_4)]$: an unusual 30-membered copper(I) cluster derived from the C-S bond cleavage and its use in heterogeneous catalysis, Chem. Commun. 49 (2013) 4259–4261.

[63] J.C. Vantourout, H.N. Miras, A. Isidro-Llobet, S. Sproules, A.J.B. Watson, Spectroscopic studies of the Chan−Lam amination: a mechanism-inspired solution to boronic ester reactivity, J. Am. Chem. Soc. 139 (2017) 4769–4779.